Research Article

Development of Solid-Contact Potentiometric Sensor Utilized Nanocarbon-filled Poly (vinyl chloride) Membrane as Ion-to-electron Transducing Layer

Turyshev ES, Shpigun LK*, Kopytin AV, Zhizhin KY, Kuznetsov NT, and Simonenko NP

N.S. Kurnakov Institute of General and Inorganic Chemistry of Russian Academy of Sciences, Russia

*Corresponding author: Liliya Shpigun

N.S. Kurnakov Institute of General and Inorganic Chemistry of Russian Academy of Sciences, Leninskii pr.31, Moscow 119991, Russia

Abstract

Current fundamental researches in the field of potentiometry demonstrate the perspectives of using polymeric nanostructured materials as ion-to-electron transducers in Solid-Contact Potentiometric Sensors (SCSs). This paper reports the preparation and comparative study of plasticized Poly(Vinyl Chloride) (PVC) membranes modified with fullerene C60, single-walled carbon nanotubes SW-CNTs, multiwalled carbon nanotubes, and graphene oxide as the transducing layer in SCSs for the determination of a common local anesthetic drug – procaine hydrochloride (Pro·HCl). As an ion-sensitive (recognizing) layer, a PVC membrane containing highly lipophilic 2-[bis-octadecyl sulfo]-closo-decaborate anions was chosen. The results were discussed in relation to nanofiller's type and content. The best potentiometric characteristics were obtained for the sensor with the transducing layer containing the hybrid nanofiller SWCNTs/C60. This new sensor of a double-layer PVC membrane configuration exhibited a Nernstian slope (59.2 ± 0.2 mV/decade) in the wide linear range ($5 \times 10^{-7} - 1 \times 10^{-2}$ M) with the low limit of detection ($10^{-7.1}$ M), fast response time (≤ 7 s), and stable potentiometric response (drift potential ± 0.27 mV h^{-1} over 7 h of soaking in 1×10^{-5} M Pro·HCl solution).

Keywords: Solid-Contact Potentiometric Sensor; Double-Layer Membrane Configuration; Poly(Vinyl Chloride) Nanostructuredmaterial; Potential Drift; Procaine Hydrochloride

Introduction

The development of inexpensive and low-energy sensors with a solid contact has become a hot topic in the field of modern potentiometry [1-7]. However, conventional potentiometric sensors like Ion-Selective Electrodes (ISEs) with an internal reference solution have a number of disadvantages, including the potential response instability and the need for frequent calibration procedure, which significantly limits their practical application [8]. The most effective approach to wearable ion potentiometric sensing appears to be the use of sensors with a solid-contact configuration [9,10].

According to the literature, a Solid-Contact Ion-Selective Electrode (SC-ISE) is an asymmetric device in which the Ion-Sensing Membrane (ISM) contacts with the electron conductor through an ion-to-electron transducer layer (instead of an internal reference solution) [11]. In most cases, such sensors are characterized by good performance parameters, portability and simplicity of construction, and the possibility of using at arbitrary electrode orientation, elevated temperature and pressure [12,13]. Moreover, their lower Limit of Detection (LOD) can be extended to the sub-nanomolar range by eliminating transmembrane ion fluxes [14]. So far, the main efforts of researchers are focused on the search for effective materials containing various ion-to-electron transducers. It is generally accepted that the following properties are required for these transducing materials [15-20]:

➢ High chemical stability;

➢ Reversibility of the transition from ionic to electronic

conductivity;

➤   Charge-transfer capability (to produce a stable potential);

➤   High degree of hydrophobicity;

➤   Absence of side reactions in the potential forming process.

To date, several groups of solid-state transducers have been proposed (Figure 1).

Important progress has been made in the fabrication of ion-to-electron transducers using carbon materials [21-31]. In principle, graphite, carbon fiber, glass carbon or carbositall directly coated with an ISM can be considered as solid-contact membrane sensors. Unfortunately, in this case the resulting EDL has a very small capacitance, which leads to a significant drift of potentiometric response during the time [32,33]. To decide this problem, it has been proposed to disperse different Carbon Nanoparticles (CNPs) directly into the ion-sensing membrane compositions [34-39]. The functionalized nanomaterials were found to be favorable for developing such type of sensors [40-42]. For example, P. Blondeau et al. [40] developed potentiometric Pb^{2+}-sensor based on benzo-18-crown-6 covalently linked to MWCNTs, which acted not only as a recognition receptor, but also as an ion-to-electron transducer. The ionophore-transducer material based on magnetic graphene hybrids and 2, 2-dithiodipyridine in La(III)-ISE was also reported [43]. F.X. Rius et al. used SWCNTs as a receptor layer to develop a potentiometric sensor for detecting neutral aromatic hydrocarbon in aqueous solutions [44]. The mechanism of the potentiometric response was based on the adsorption of aromatic hydrocarbons on the side walls of the SWCNTs through hydrophobic interactions and π-π-stacking, which leads to a change in the interfacial capacity of the EDL between SWCNTs and the sample solution. However, the dispersion of conducting nanofillers in the heterogeneous ISM is critical for its potentiometric selectivity. Therefore, significant research efforts are focused on the development of sensors containing carbon nanomaterial-based intermediate layers between ISMs and solid conductors. Various types of CNPs-based solid contacts have been proposed (Table 1).

In recent years, an understanding of the ion-to-electron transduction mechanism of CNPs has led to significant improvements in the performance of SCSs [5-9]. Remarkable examples of carbon-modified Conducting Polymers (CPs) as mixed-mode transducers have been reported [59-61,74,75,85,86]. Such materials combining polymer continuous phase and CNPs as discontinuous phase showed several advantages compared with individual components, such as a significant increase in the EDL capacity at the interface between the SC-layer and the ISM and a faster charge transfer. However, CPs can have drawbacks such as high electroactivity that generates interfering processes. From our point of view, polymeric nanomaterials, represented in the form of non-conductive polymeric membranes of a three-dimensional nanostructure, also seem to be promising materials for the solid-contact fabrication. Of particular interest is the use of polar polymer Poly(Vinyl Chloride) (PVC) modified with CNPs, which provide the formation of densely packed interfacial regions and, as a consequence, the change in the structural characteristics of the polymer matrix. According to the literature, PVC is the most suitable polymer for segregated composites, due to its high viscosity and wide temperature range of

softening (due to its amorphous structure). Nevertheless, the research works devoted to CNPs-filled PVC materials are carried out not long ago. Several studies have been conducted to the dispersion of nanofillers in polymer matrices [87-94]. For example, G. Broza et al. prepared PVC composites with multi- and single-walled CNTs in tetrahydrofuran followed by film casting. They reported the conductivity of 5×10^{-3} S cm^{-1} for PVC-MW-CNTs composite containing 5 wt.% CNTs [88]. Recently, PVC/mixed graphene-carbon nanotube nanocomposites have been proposed as a selective amperometric Ag^+-sensor [92]. Y. Liu et al. described a single-piece solid contact Pb^{2+}-selective electrode with MWCNTs directly dispersed in the NPOE-plasticized PVC membrane [38].

The mechanism of the carbon nanomaterials functioning in the SC-ISes has yet to be studied in detail. By analogy with the ion-sensitive field-effect transistors, their behavior as ion-to-electronic transducers may be due to electrostatic coupling: the presence of charged ions in an ion-sensitive membrane in close contact with a CNPs-based layer may provide electronic capacitive coupling [95]. To this connection, the electrode response is determined by the sum of the potentials of the following three interfaces (interphase potentials): conductor/SC ($\Delta\phi c_1$), SC/ISM ($\Delta\phi c_2$), and ISM/solution ($\Delta\phi c_3$). According to the phase-boundary model of ISEs [96], the interfacial potential $\Delta\phi c_3$ is based on the assumption of local equilibria at the aqueous solution/ISM interface. The potential jump $\Delta\phi c_1$ at the conductor/SC interface is usually very small, since carbon nanomaterials used have a high electronic conductivity. The potential jump $\Delta\phi c_2$ at the SC/ISM interface can be described as an asymmetric electrical capacitor, in which one side transfers is a charge in the form of ions, i.e. cations and anions from the ion-sensing membrane, and the other side is formed by electrical charges, i.e. electrons or holes in the SC-layer. In a word, the ion-to-electron transduction process is the result of the EDL formation at the SC/ISM interface [97]. This mechanism is largely determined by the distribution of nanoparticles in the volume of SC-layer, their interaction with the polymer matrix and with each other, and the diffusion of nanoparticles in the composite. It should be noted, however, that not only the interface $\Delta\phi c_2$ but also all other interfacial potentials have to be controlled to ensure the e.m.f. stability. In moderately accurate potentiometric measurements, an acceptable potential drift is assuming to be 1.0 mV·h^{-1} that corresponded to a minimal electrode capacitance of 3.6 µF (at a residual current of 1 pA) [4].

Building on these general considerations, we studied of a series of the CNPs immobilized in plasticized PVC membranes in terms of their use as a SC-interlayer in potentiometric membrane sensors. Our goal was to compare the fabricated systems through examining the electroanalytical characteristics of the sensor for the determination of cationic forms of procaine hydrochloride (or novocain, 2-diethyl-aminoethyl-4-aminobenzoate hydrochloride) with local anesthetic and antiarrhythmic properties. As ISM, a plasticized PVC membrane incorporating ion-exchange salt of protonated procaine cations with 2-[bis-octadecyl-sulfonic]-*closo*-decaborate anions (ProH[$B_{10}H_9S$(n-$C_{18}H_{37})_2$]) was used [98].

Materials and Methods

Reagents and Solutions

High molecular weight PVC, Bis(1-Butylpezntyl)Adipate (BBPA), procaine hydrochloride (Pro·HCl, 99 %, p/p purity) were purchased from Merck KGaA and used without prior

purification. Tetrahydrofuran (THF) was distilled before use. $Cs[B_{10}H_9S(n-C_{18}H_{37})_2]$, which was synthesized and identified in the laboratory of chemistry of light elements and clusters of the N.S. Kurnakov institute of General and Inorganic Chemistry of RAS [99]. The procaine hydrochloride stock solutions (0.1 M and 1000 µg mL^{-1}) was prepared by dissolving a precise amount of the compound in water or in 0.01 M HCl-NaOH solution. The working standard solutions with concentrations of 10^{-2}— 10^{-8} M were prepared daily from the stock solution by serial dilution. All reagents and chemicals used throughout this work were of analytical-reagent grade and solutions were prepared with re-distilled water (resistivity > 18 MΩ·cm^{-1}). All solutions were re-frigerated between uses.

Sensor Preparation Procedures

In order to prepare PVC-based nanocomposite membranes, the commercially available fullerene C60 (99.5%, Bucky USA), SWCNTs (> 90 %, 0.7–0.9 nm diameter, Aldrich), cleaned MW-CNTs (95%, Bucky USA), and GO (powder, Aldrich) were used. Here, PVC plays the role of dispersing material for CNPs in the suspension. To achieve a homogeneous distribution of carbon nanofillers in the plasticized PVC matrix, a two-stage proce-dure was used. The first stage involved 10 – 30% PVC solutions preparation by mechanically stirred PVC powder and plasticiz-er BBPA in freshly distilled THF for 3 h at 30°C. In the second stage, the required amount of the plasticized polymer solution was mixed with CNPs to obtain suspensions containing differ-ent weight fractions of nanofillers (2–20 wt.%). The CNPs-PVC suspensions were prepared with the aid of ultrasonic agitation during 30 – 40 min.

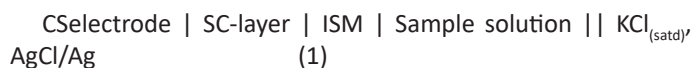The ion-exchange salt of protonated procaine cation with a high lipophilic 2-[bis-octadecyl-sulfonic]-*closo*-decaborate an-ion ($ProH[B_{10}H_9S(n-C_{18}H_{37})_2]$)was synthesized and identified as it has been previously reported (Figure 2) [98].

The ISM precursor solution of the following composition (wt.%) was prepared: electroactive compound $ProH[B_{10}H_9S(n-C_{18}H_{37})_2]$– 1.2; plasticizer (BBPA) – 68.8; PVC – 30.0. The com-ponents were dissolved in 2.0 mL dry freshly distilled THF. Af-ter the membrane cocktail was homogeneously mixed, it was stored at 4°C.
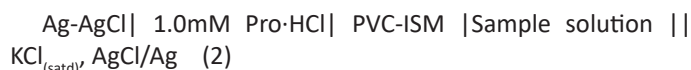
All investigating doble-layer PVC membrane sensors were fabricated using a substrate Carbositall (CS) electrode (Wolta, Russia). Prior to use, the polished and ultrasonically irradiated CS electrode was electrochemically activated in 0.1 M HClO$_4$ by scanning potential in the range of (0.0 – +1.4) V for 20 cycles (voltage scan rate v = 0.05 V s^{-1}). Finally, 20 µL of the corre-sponding PVC-based nanocomposite suspension (in 10 µL ali-quots) was applied onto the CS surface. After drying at 34°C in a pressure chamber, the modified CS electrode was coated with a ISM precursor solution(in two portions of 25 µL) to form the potentiometric sensor with two PVC membranes(named as SC-ProH$^+$-ISE). For comparison, a solvent polymeric membrane ISE with an inner solution (named as ProH$^+$-ISE) was fabricated in accordance with the procedure described early [98], and then mounted in an electrode body (Type IS 561, Philips, Eindhoven, Netherlands) filled with 1.0 mM Pro·HCl. The prepared sensors were placed into 1.0×10^{-3} M Pro·HCl solution for 24 h, and then stored in the air without sunlight. Before using, each electrode was conditioned in 1.0×10^{-7} M Pro·HCl solution.

Instrumentation

The following experiments were performed to characterize the SC-ISEs: SEM morphological observation; cyclic voltammet-ric and potentiometric measurements at the room temperature (23 ± 2°C). All potentiometric measurements were carried out by using a pH/ion analyzer Radelkis OP-300 «Hungary». The cell's e.m.f. (E_{cell}) were recorded using the following galvanic cir-cuit:

CSelectrode | SC-layer | ISM | Sample solution || KCl$_{(satd)}$, AgCl/Ag   (1)

An electrochemical cell set up of the conventional ProH$^+$-ISE was as follows:

Ag-AgCl| 1.0mM Pro·HCl| PVC-ISM |Sample solution || KCl$_{(satd)}$, AgCl/Ag   (2)

Cyclic voltammetric experiments were carried out with an Ecotest-VA Analyser (Econix-Expert, Russia) interfaced to a com-puter system with MDEV software. A three-electrode cell was used, where a modified CSE served as the working electrode, an Ag/AgCl, KCl$_{(satd)}$ and a platinum wire served as the reference electrode and the auxiliary electrode, respectively. The com-puter program Origin 2017 based on the Levenberg–Marquardt algorithm was used for signal processing and peak analysis. The surface morphology of CNPs and prepared polymeric compos-ites was examined with a scanning electron microscope (SEM, Carl Zeiss NVision 40, Germany). pH values were tested by using a pH-meter Model OP-110 (Radelkis, Hungary). The ultrasonic bath (Elmasonic One, Germany, 35-kHz ultrasound) was used in all ultrasonic procedures.
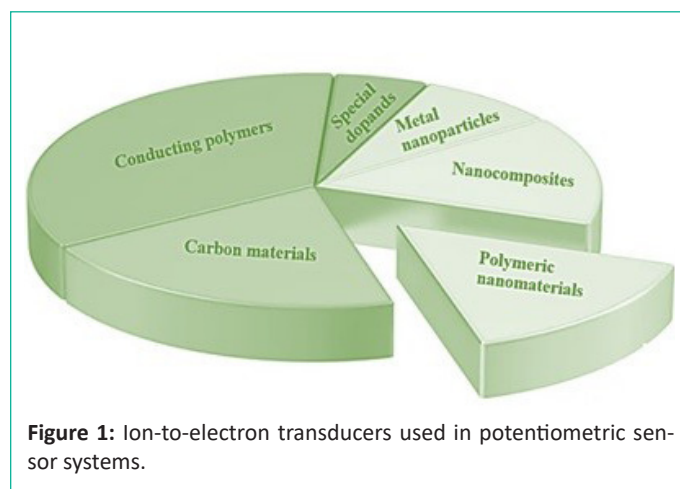

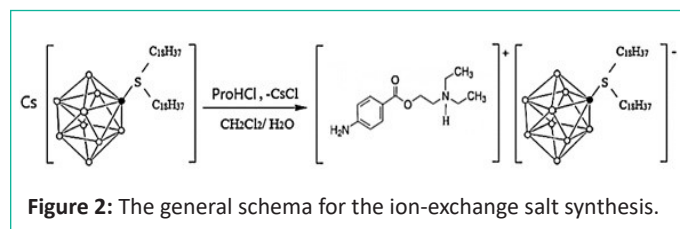**Figure 1:** Ion-to-electron transducers used in potentiometric sen-sor systems.

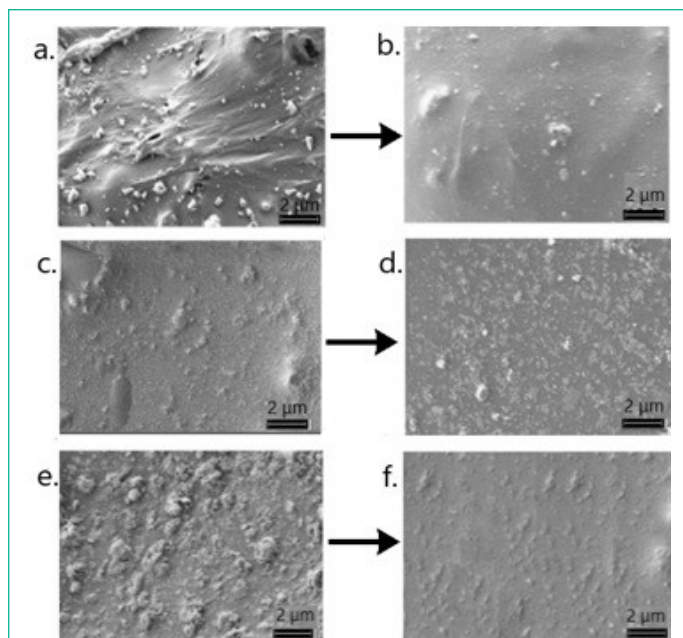**Figure 2:** The general schema for the ion-exchange salt synthesis.

Figure 3: SEM images of the plasticized PVC matrices modified with SWCNT **(a,b)**, fullerene C60 **(c,d)**, and hybrid SWCNT-C60 **(e,f)** before **(a,c,e)** and after **(b,d,f)** ultrasonication.
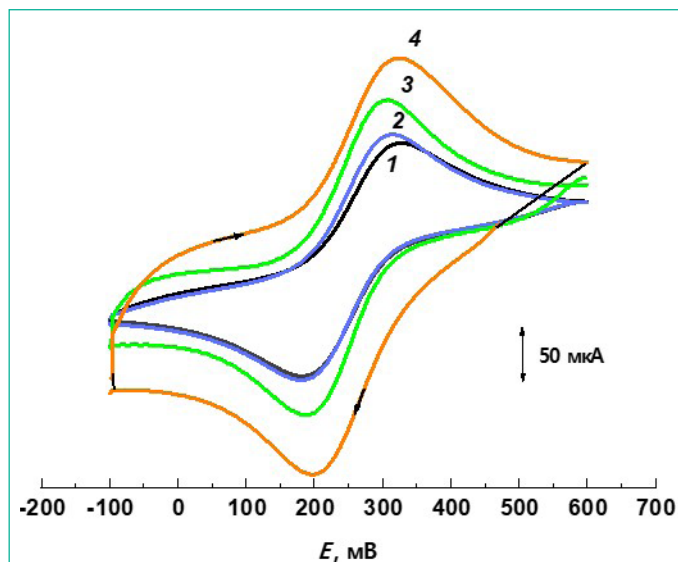

Figure 4: Cyclic voltammetric curves obtained for the CNPs-dopped film modified SCE in 1.0 M KCl solution containing 5.0 mM of $Fe(CN)_6^{3/4}$ (scan rate – 100 mVs^{-1}). CNPs: 1 – GO; 2 – C60; 3 – SW-CNTs; 4 – MWCNTs.

Table 1: List of the reported SC-ISEs containing nanocarbon-based transducer layers.

Ion-to-electron transducer	Primary ion	E.m.f. drift, mV·h^{-1} (1 nA appl., μV·s^{-1})	LOD, M	Reference
Fullerene C$_{60}$ and derivatives	K$^+$	85.0	$10^{-5.4}$	[45–47]
Bimodal pore C60	Pb^{2+}	(11.0)	$10^{-9.3}$	[48]
SWCNTs	K$^+$	(17.0)	$10^{-5.5}$	[49]
SWCNTs	Ca^{2+}	493	$10^{-6.2}$	[50]
SWCNTs-ODA	K$^+$	0.19	$10^{-6.6}$	[51]
MWCNTs -Octamide	Choline	0.05	$10^{-6.4}$	[52]
MWCNTs loaded epoxy resin MWCNTs–COOH	Cu^{2+}	Nr	$10^{-8.0}$	[53]
Carboxylated MWCNTs	Paroxetine	Nr	$10^{-7.1}$	[54]
Lipophilic MWCNTs	ClO$_4^-$	0.22	$10^{-7.4}$	[55]
Octadecane-modified CNTs	CO$_3^{2-}$	0.04	$10^{-5.6}$	[56]
Ferrocene- modified MWCNTs	K$^+$	< 0.8	$10^{-6.3}$	[57]
MWCNTs – POT	K$^+$	Nr	$10^{-6.4}$	[58]
MWCNTs – PEDOT	K$^+$	≈ 0.1	$10^{-6.8}$	[59]
MWCNTs/PA	K$^+$	12.0	$10^{-6.0}$	[60]
MWCNTs -ETH500	Pb^{2+}	Nr	$10^{-9.5}$	[61]
MWCNTs-COOH	NO$_2^-$/NO$_3^-$	(17.0)	$10^{-7.5}$	[62]
Au/Cu NPs-MWCNTs	HPO$_4^{2-}$	Nr	$10^{-6.7}$	[63]
Graphene sheets	Ca^{2+}/ SO$_4^{2-}$	0.015/0.118	$10^{-6.2}$/$10^{-5.0}$	[64]
Defect-free graphene sheets	K$^+$	8.4	$10^{-5.5}$	[65]
rGO	K$^+$	0.74	$10^{-4.3}$	[66]
G – AgTFPB	K$^+$	(12.8)	$10^{-6.2}$	[67]
G–carbon black-fluoropolymer	K$^+$	12.6	$10^{-5.7}$	[68]
Carboxy-functionalized G	K$^+$	1.0	$10^{-6.7}$	[69]
Thiol-functionalized rGO	K$^+$	Nr	$10^{-7.1}$	[70]
rGO	K$^+$/ NO$_3^-$	(1.75/ 8.79)	$10^{-5.6}$/$10^{-5.4}$	[71]
Electrochemically rGO	Ca^{2+}	0.9	$10^{-6.2}$	[72]
G/PANI	Ca^{2+}	0.13	$10^{-5.8}$	[73]
GO/PPY	Ca^{2+}	0.2	$10^{-7.3}$	[74]
rGO-coated black phosphorus	Ca^{2+}	(10.0)	$10^{-6.6}$	[75]
rGO aerogel	Ca^{2+}	0.01	$10^{-5.1}$	[76]
G-tetrathiafulvalene	Ca^{2+}	0.03 / 0.06	$10^{-6.7}$/$10^{-6.1}$	[77]
G	Ca^{2+} / NO$_3^-$	(4.26)	$10^{-6.2}$	[78]
rGO	NO$_3^-$	Nr	$10^{-4.3}$	[79]
r-GO/Ag@AgCl/TMMCl	NO$_3^-$	(< 2.86)	$10^{-5.4}$	[80]
SWCNHs	Br$^-$	0.12 (43.0)	$10^{-6.1}$	[81]
SWCNTs-ETH 500	Ca^{2+}	Nr	$10^{-6.0}$	[82]
Carbon nanofiber-PVC	Ca^{2+}	0.35	$10^{-8.4}$	[83]
	Cu^{2+}	(0.04)	$10^{-6.8}$	[84]
	Moxifloxacin enantiomers			

SWCNTs – single-walled carbon nanotubes; MWCNTs – multi-walled carbon nanotubes; G – graphene; GO – graphene oxide; rGO – reduced graphene oxide; SWCNHs – single-walled carbon nanohorns; POT – poly(3-octylthiophene-2,5-diyl); PPY – polypyrrole; PEDOT – poly(3,4-ethylenedioxythiophene; AgTFPB – silver tetrakis[3,5-bis(trifluoro-methyl)phenyl]borate; ODA – octadecylamine; PA – polyaniline; DTDP–2,2-dithiodipyridine; ETH500 – tetradodecylammonium tetrakis (4-chlorophenyl) borate, TMMCl – 1-tetradecyl-3-methylimidazolium chloride; Nr – not reported.
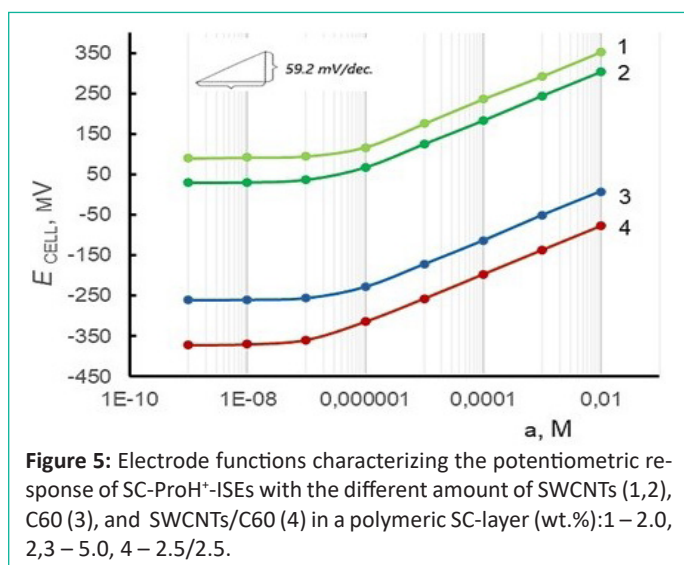

Figure 5: Electrode functions characterizing the potentiometric response of SC-ProH$^+$-ISEs with the different amount of SWCNTs (1,2), C60 (3), and SWCNTs/C60 (4) in a polymeric SC-layer (wt.%):1 – 2.0, 2,3 – 5.0, 4 – 2.5/2.5.

Table 2: Selected electrochemical characteristics of CNPs-dopped film modified CSE obtained using quasi-reversible redox-probe [Fe(CN)$_6$]$^{3-/4-}$(v = 0.1 V s^{-1}).

Carbon nanofiller	Q, mm^2(n=5)	ΔE_p, mV	E^o, V
–	4.9 ± 0.1	206	0.253
C60	12.5 ± 0.2	147	0.254
SWCNTs	14.4± 0.5	138	0.249
MWCNTs	18.3± 0.4	125	0.245
GO	11.6 ± 0.3	154	

Table 3: Electrode response performance of the fabricated SC-ISEs for the ProH$^+$-ions determination (n=5).

Nanofiller (5 wt. %)	E_o', мB	Slope, mV·dec.$^{-1}$	Linear range, M	LOD, M	Response time, τ_{95} (≥ 1×10^{-6} M)
SWCNTs	421.7	59.2 ± 0.2	9×10^{-7} – 1×10^{-2}	10$^{-6.52}$	10
MWCNTs	450.8	59.3 ± 0.3	9×10^{-6} – 1×10^{-2}	10$^{-6.46}$	9
GO	446.9	58.9 ± 0.4	1×10^{-6} – 1×10^{-2}	10$^{-6.30}$	14
C60	124.8	59.0± 0.3	1×10^{-6} – 1×10^{-2}	10$^{-6.40}$	12

Results and Discussion

Performance Evaluation of CNPs-filled PVC Membranes

Many aspects of nanoparticle diffusion in the PVC during the composite formation are still far from being solved. By now, it has been established that the CNPs incorporation into a PVC solution leads to the stretching of macromolecules of the polymer, and the formation of a tightly packed inter phase layer CNPs-polymer. Localized nanoparticles can form an ordered network of conductive phases, creating so-called segregated systems. The self-aggregation or rearrangement of carbon nanoparticles due to strong van der Waals interactions lead to changes of the effective surface area and the electrical conductivity of composites. Evidently, to generate electrically conductive paths in the polymeric matrix, the agglomerates of CNPs have to be split and spread homogeneously in the PVC film [87,88]. The literature review in this field showed that an effective way to achieve a high degree of homogeneity of the polymeric nanocomposite material is the use of ultrasonic processing [92,100].
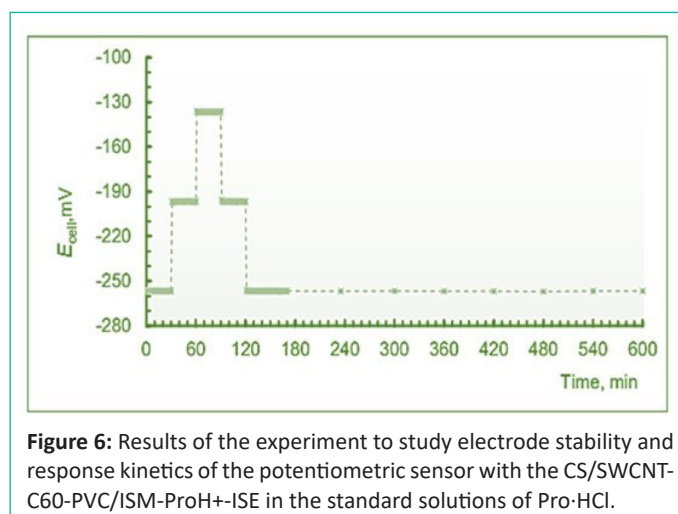

Figure 6: Results of the experiment to study electrode stability and response kinetics of the potentiometric sensor with the CS/SWCNT-C60-PVC/ISM-ProH+-ISE in the standard solutions of Pro·HCl.

Table 4: Comparison of the characteristic features of CS/SWCNT-C60-PVC/ISM-ProH$^+$-ISE with those of the previously reported solvent polymeric membrane ProH$^+$-ISE (n=5).

Parameter	CS/SWCNT-C60-PVC/ProH$^+$-ISE	ProH$^+$-ISE with an inner solution
Slope (s), mV/decade	58.9 ± 0.2	58.1 ± 0.5
E_o', mV	40.8 ±0.3	303.7 ± 2.4
Correlation coefficient, R^2	0.9998	0.9996
Linear range	5×10^{-7} – 1×10^{-2}	1×10^{-6} – 1×10^{-2}
Limit of detection, M	10$^{-7.05}$	10$^{-6.02}$
pH-range	2.5–8.1	2.7 – 8.2
Response time,t_{95}, s (1.0 µM)	7 ± 1	20 ± 2
$\log K^{pot}_{ProH^+/j}$:		
Li$^+$	-3.1 ± 0.3	-3.2 ± 0.4
Na$^+$	-3.0 ± 0.2	-3.1 ± 0.3
K$^+$	-3.1 ± 0.2	-3.0 ± 0.1
Rb$^+$	-3.2 ± 0.1	-3.1 ± 0.2
Cs$^+$	-3.8 ± 0.3	-3.9 ± 0.4
Ca^{2+}	-3.8 ± 0.3	-3.8 ± 0.4
Sr^{2+}	-3.7 ± 0.2	-3.8 ± 0.3
Ba^{2+}	-3.9 ± 0.4	-3.7 ± 0.3
NH$_4^+$	-3.6 ± 0.2	-2.7 ± 0.1
Glycine	-2.8 ± 0.2	-2.7 ± 0.1
Valine	-3.0 ± 0.3	-2.8 ± 0.2
β-Alanine	-3.1 ± 0.1	-3.0 ± 0.2
Urea	-3.0 ± 0.2	-3.2 ± 0.3
Fructose	-3.9 ± 0.3	-3.8 ± 0.4
Glucose	-3.8 ± 0.3	-3.9 ± 0.5
Sucrose	-4.2 ± 0.4	-4.1 ± 0.5

Since the potentiometric response of SCSs is related to the physical properties of SC-layers, we investigated the surface morphology of CNPs–PVC composite membranes before and after ultrasonication (Figure 3). SEM observation of the prepared composite materials without ultrasonication showed that the nanofillers distribution in the plasticized PVC-matrix was heterogeneous (Figure 3a,c,e). The aggregated CNPs may be visible, especially in the areas of interstructural defect zones in PVC. The powerful ultrasonic treatment leaded to formation of micelles, which can be single nanostructures or small diameter bundles surrounded by plas-

ticizer molecules (Figure 3b,d,f). The plasticizer probably serves as a carrier of nanoparticles for their distribution within the PVC matrix, which results changes in the conditions of interaction between the polymer and nanofillers [101]. The most uniform distribution of nanofillers was observed in the case of hybrid C60-SWCNTs. It can be expected that the concurrent usage of both fillers can effectively stop aggregation and achieve good dispersion in the polymer matrix.

In order to get an insight into the role of CNPs-PVC composite membrane in the potentiometric response of the prepared SC-ISEs, we investigated redox processes of a redox-probe $[Fe(CN)_6]^{3-/4-}$ at the modified CS electrode (CSE) by cyclic voltammetry with a potential scan rate v between 0.025 and 0.200 $V \cdot s^{-1}$ (Figure 4). It was found that the PVC membrane coated electrode shows no redox sensitivity because the PVC is an electronic insulator (0.004×10^{-5} S cm^{-1}), and the electrical conductivity on the CNPs-PVC composite materials depends significantly on the nanofiller concentration. We performed redox measurements using a CSE covered with a film containing 20 wt.% CNPs. The results indicated that the modifying layer formed on the SCE surface provided a significant increase in the measurable cathodic and anodic peaks, which is mainly due to increasing the electroactive surface area of the modified CSE (Q) compared to the pure surface. The dependence of peak current values and $v^{1/2}$ was linear, which corresponds to the course of electrochemical processes limited to the semi-infinite linear diffusion of reactants to the electrode surface. The relatively slow electron transfer kinetics and high background current may be related to the surface structure of the modifying film. However, it can be expected that in all cases the CNTs network was formed, which provided electrical conductivity of the films. The Q values calculated according to the Randles-Shevchik equation [102] and other selected characteristics are given in (Table 2).

According to the findings, all of the studied materials are characterized by a queasy-reversible redox capacity and a sufficiently large electroactive surface area. However, one should take into account the peculiarities of electrochemical processes within the nanostructured films, which are caused not only by their large specific surface area [103].

Potentiometric Characteristics of Double-Layered Membrane Sensors

Key potentiometric characteristics of the fabricated SC-ISEs, such as sensitivity, selectivity, reversibility, medium-term stability and reproducibility, were evaluated by using their response towards ProH$^+$-ions. As it can be concluded from the (Table 3), all sensors provided the operational Nernstian response slope within 0.5 % of the theoretical valuefor single-charged ions (s = 59.2 mV·dec.$^{-1}$, 25°C) within the wide range of the ProH$^+$activity (a_i):

$$E_{cell} = E_o' + \log a_i \qquad (3)$$

It is obvious that their response towards ProH$^+$ is mainly determined by the ion-sensing membrane composition. However, the nature and concentration of CNPs in the transducer layer has a remarkable influence on the cell's e.m.f. (i.e., apparent standard potential E_o'), which is mainly due to changes in the value of the SC/ISM interfacial jump potential. The best response characteristics were obtained for sensors fabricated using the intermediate layer with 5.0 wt.% of a nanofiller. A further increase in the nanofiller's amount in the transducing membrane was accompanied by a noticeable shift of the elec-

trode function to the region of less positive values, as well as by a deterioration of the potentiometric parameters. The observed effect can be attributed to the increased aggregation of nanofiller molecules in the PVC film during preparing the composite solution and forming the SC-layer on the surface of the substrate electrode. LOD of ProH$^+$ cations were also found to be dependent on the SC-layer composition.

It is noteworthy that E_o' for the sensor containing PVC membrane filled with nanomolecules of fullerene C60 is significantly lower than in the other cases (Figure 5). This may be attributed to the special properties of this nanomaterial, in particular with the ability of magical fullerene nanoclusters to non-covalent binding with the plasticized polymer [89]. Further research has shown that the combination of two nanofillers – SWCNTs and C60 yields a significant reduction in the E_o' values compared to their counterparts based on SWCNT-PVC or C60-PVC intermediate membranes. It can be suggested that non-covalently attached fullerenes are highly mobile on the surface of SWNTs and, being effective charge transfer mediators, can reversibly accept several electrons and form stable intermediate multianions, while SWCNTs can serve for setting high-mobility pathways for electron transport [104-107].

Importable, the sensor with the SC-layer containing the hybrid nanofiller SWCNT/C60 (designated as CS/SWCNT-C60-PVC/ProH$^+$-ISE) demonstrates faster response time, greater linear detection range, and lower LOD with respect to procaine cations than other manufactured sensors, including its counterpart with internal reference solution (Table 4).

The potentiometric response stability and reversibility of the newly fabricated CS/SWCNT-C60-PVC/ProH$^+$-ISE was confirmed by initially placing the electrode in 1×10^{-5} M procaine hydrochloride solution. After 1.0 h, this solution was subsequently replaced by more concentrated solutions: 1×10^{-4} M and 1×10^{-3} M. Then, a similar procedure in the opposite direction was carried out (Figure 6). It was found that the potential drift of the prepared sensor during conditioning in 1×10^{-5} M Pro·HCl was usually ± 0.27 mV h^{-1} over 7 h of soaking. It should be noted that among different causes of $e.m.f.$ drift, the formation of a water layer between the ISM and the SC-layer is supposed to play a crucial role [108,109]. However, in our case the uptake of water is apparently needed for reaching stable electrode potentials and advantageous for proper operating of the electrode [110,111]. The new CS/SWCNT-C60-PVC/ProH$^+$-ISE sensor showed very good reproducibility of the electrode function slope and the formal standard potential. The standard deviation values of the linear response slope of ± 0.25 mV dec^{-1} and E_o' of ± 0.49 mV were observed during 7 days.

The selected results of the analysis of pharmaceutical injections of Pro·HCl are shown in Table 5. As it can be seen, the analyte concentrations determined by the proposed sensor were very similar to the label values, and the recoveries of all tested samples were almost quantitative.

Overall, the presented here potentiometric properties of the new sensor allow us to conclude that the hybrid nanocarbon material in PVC modification appears to be an excellent candidate for the role of an ion-to-electron transducer in SC-ISEs.

Conclusion

Solid-contact membrane sensors are of increasing interest for wearable potentiometric analysis. Combination of nanotechnology with recent progress in supramolecular chemistry

and electroanalysis is leading to improved ion-sensing strategies. Polymers containing CNPs as nanofillers are next-generation smart materials to fabricate advanced ISEs. In this paper we have demonstrated CNPs-PVC membranes as a class of materials with a great deal of promise for applications as ion-to-electron transducers in polymeric membrane sensors. The above results showed that a novel double-layer PVC membrane-based sensor containing a hybrid carbon filler (SWCNTs and C60) as an ion-to-electron transducer is characterized by remarkable reproducibility of the electrode function slope and improved stability of the potentiometric response towards procaine cations. This sensor can be recommended for the daily routine quantitation of procaine in pure forms and pharmaceuticals.

Conflict of Interest

The authors declare no conflict of interest

References

1. Bakker E, Pretsch E. Modern potentiometry. Angew. Chemie Int. Ed. 2007; 46: 5660–5668.

2. Pretsch E. The new wave of ion-selective electrodes. TrAC Trends Anal. Chem. 2007; 26: 46–51.

3. Hu J, Stein A, Bühlmann P. Rational design of all-solid-state ion-selective electrodes and reference electrodes. TrAC Trends Anal Chem. 2016; 76: 102–114.

4. Bieg C, Fuchsberger K, Stelzle M. Introduction to polymer-based solid-contact ion-selective electrodes–basic concepts, practical considerations, and current research topics. Anal Bioanal Chem. 2017; 409: 45–61.

5. Shao Y, Ying Y, Ping J. Recent advances in solid-contact ion-selective electrodes: functional materials, transduction mechanisms, and development trends. Chem Soc Rev. 2020; 49: 4405–4465.

6. Lyu Y, Gan S, Bao Y, Zhong L, Xu J, Wang W, et al. Solid-contact ion-selective electrodes: response mechanisms, transducer materials and wearable sensors. Membranes (Basel). 2020; 10: 128.

7. Maksymiuk K, Stelmach E, Michalska A. Unintended changes of ion-selective membranes composition–origin and effect on analytical performance. Membranes (Basel). 2020; 10: 266.

8. Buck RP. Theory and principles of membrane electrodes. H. Freiser (Ed.) In: Ion-Selective Electrodes in Anal. Chem. Boston. 1978; 1–141.

9. Parrilla M, Cuartero M, Crespo GA. Wearable potentiometric ion sensors. TrAC Trends Anal. Chem. 2019; 110: 303–320.

10. Yeung KK, Li J, Huang T, Hosseini II, Mahdi R Al, Alam Md M, et al. Utilizing gradient porous graphene substrate as the solid-contact layer to enhance wearable electrochemical sweat sensor sensitivity. Nano Lett. 2022; 16: 6647–6654.

11. Cadogan A, Gao Z, Lewenstam A, Ivaska A, Diamond D. All-solid-state sodium-selective electrode based on a calixarene ionophore in a poly(vinyl chloride) membrane with a polypyrrole solid contact, Anal. Chem. 1992; 64: 2496–2501.

12. Cheong YH, Ge L, Lisak G. Highly reproducible solid contact ion selective electrodes: emerging opportunities for potentiometry – a review. Anal Chim Acta. 2021; 1162: 338304.

13. Huang MR, Li XG. Highly sensing and transducing materials for potentiometric ion sensors with versatile applicability, Prog Mater Sci. 2022; 125: 100885.

14. Sutter J, Lindner E, Gyurcsányi R, Pretsch E. A polypyrrole-based solid-contact Pb2+-selective PVC-membrane electrode with a nanomolar detection limit. Anal. Bioanal Chem. 2004; 380: 7–14.

15. Nikolskii BP, Materova EA. Solid contact in membrane ion-selective electrodes. Leningrad. 1985.

16. Lindner E, Gyurcsányi RE. Quality control criteria for solid-contact, solvent polymeric membrane ion-selective electrodes. J. Solid State Electrochem. 2009; 13: 51–68.

17. Ivanova NM, Levin MB, Mikhelson KN. Problems and prospects of solid contact ion-selective electrodes with ionophore-based membranes. Russ Chem Bull. 2012; 61: 926–936.

18. Bobacka J, Ivaska A, Lewenstam A. Potentiometric ion sensors. Chem Rev. 2008; 108: 329–351.

19. Michalska A. All-solid-state ion selective and all-solid-state reference electrodes. Electroanalysis. 2012; 24: 1253–1265.

20. John B. Polymer nanocomposite-based electrochemical sensors and biosensors. Nanorods and nanocomposites. 2020.

21. Yin T, W. Qin W. Applications of nanomaterials in potentiometric sensors. TrAC Trends Anal. Chem. 2013; 51: 79–86.

22. Zhang Y, Tang Y, Liang R, Zhong L, Xu J, Lu H, et al. Carbon-based transducers for solid-contact calcium ion-selective electrodes: mesopore and nitrogen-doping effects. Membranes. 2022; 12: 903.

23. Lai CZ, Fierke MA, Stein A, Bühlmann P. Ion-selective electrodes with three-dimensionally ordered macroporous carbon as the solid contact. Anal Chem. 2007; 79:4621–4626.

24. Paczosa-Bator B, Cabaj L, Piech R, Skupień K. Potentiometric sensors with carbon black supporting platinum nanoparticles. Anal Chem. 2013; 85: 10255–10261.

25. Ye J, Li F, Gan S, Jiang Y, An Q, Zhang Q, Niu L. Using sp2-C dominant porous carbon sub-micrometer spheres as solid transducers in ion-selective electrodes. Electrochem Commun. 2015; 50: 60–63.

26. Hu J, Zou XU, Stein A, Bühlmann P. Ion-selective electrodes with colloid-imprinted mesoporous carbon as solid contact. Anal Chem. 2014; 86: 7111–7118.

27. Cuartero M, Crespo GA. All-solid-state potentiometric sensors: a new wave for in situ aquatic research. Curr Opin Electrochem. 2018; 10: 98–106.

28. Jiang Z, Xi X, Qiu S, Wu D, Tang W, Guo X, Su Y, Liu R. Ordered mesoporous carbon sphere-based solid-contact ion-selective electrodes. J Mater Sci. 2019; 54: 13674–13684.

29. Jiang T, Yin B, Liu X, Yang L, Pang H, Song J, Wu S. Porous carbon-based robust, durable, and flexible electrochemical device for K+ detection in sweat. Analyst. 2022; 147: 1144–1151.

30. Wang S, Zhong L, Gan S, Tang Y, Qiu S, Lyu Y, Ma Y, Niu L. Defective vs high-quality graphene for solid-contact ion-selective electrodes: effects of capacitance and hydrophobicity. Electro-

chem. Commun. 2021; 129: 107091.

31. Ozer T, Henry CS. All-solid-state potassium-selective sensor based on carbon black modified thermoplastic electrode. Electrochim Acta. 2022. 404: 139762.

32. Hansen EH, Lamm CG, J. Růžička J. Selectrode®–the universal ion-selective solid-state electrode. Anal Chim Acta. 1972; 59: 403–426.

33. Fibbioli M, Morf WE, Badertscher M, de Rooij NF, Pretsch E. Potential drifts of solid-contacted ion-selective electrodes due to zero-current ion fluxes through the sensor membrane. Electroanalysis. 2000; 12: 1286–1292.

34. Andrade FJ, Blondeau P, Macho S, Riu J, Rius FX. Potentiometric nanostructured sensors.In: Encycl. Anal. Chem. UK: John Wiley & Sons, Ltd, Chichester. 2014; 1–17.

35. Zhu J, Li X, Qin Y, Zhang Y. Single-piece solid-contact ion-selective electrodes with polymer–carbon nanotube composites. Sens. Actuat. B Chem. 2010; 148:166–172.

36. Wardak C. Solid contact cadmium ion-selective electrode based on ionic liquid and carbon nanotubes. Sens Actuat B Chem. 2015; 209: 131–137.

37. Birinci A, Eren H, Coldur F, Coskun E, Andac M. Rapid determination of trace level copper in tea infusion samples by solid contact ion selective electrode. J Food Drug Anal. 2016; 24: 485–492.

38. Liu Y, Liu Y, Gao Y, Wang P. A general approach to one-step fabrication of single-piece nanocomposite membrane based Pb2+-selective electrodes. Sens. Actuators B Chem. 2019; 281: 705–712.

39. Mostafa SM, Farghali AA, Khalil MM. Novel Zn-FeLDH/MWCNTs and graphene/MWCNTs nanocomposites based potentiometric sensors for benzydamine determination in biological fluids and real water samples. Electroanalysis. 2021; c33: 1194–1204.

40. Parra EJ, Blondeau P, Crespo GA, Rius FX. An effective nanostructured assembly for ion-selective electrodes. An ionophore covalently linked to carbon nanotubes for Pb2+ determination. Chem Commun. 2011; 47: 2438–2440.

41. Kerric G, Parra EJ, CrespoGA, Rius FX, Blondeau P. Nanostructured assemblies for ion-sensors: functionalization of multi-wall carbon nanotubes with benzo-18-crown-6 for Pb2+ determination. J Mater. Chem. 2012; 22: 16611.

42. Parra EJ, Rius FX, Blondeau P. A potassium sensor based on non-covalent functionalization of multi-walled carbon nanotubes. Analyst. 2013; 138: 2698.

43. Yuan X, Chai Y, Yuan R, Zhao Q. Improved potentiometric response of solid-contact lanthanum (III) selective electrode. Anal Chim Acta. 2013; 779: 35–40.

44. Washe AP, Macho S, Crespo GA, Rius FX. Potentiometric on-line detection of aromatic hydrocarbons in aqueous phase using carbon nanotube-based sensors. Anal Chem. 2010; 82: 8106–8112.

45. Fibbioli M, Enger O, Diederich F, Pretsch E, Bandyopadhyay K, Liu SG, et al. Redox-active self-assembled monolayers as novel solid contacts for ion-selective electrodes. Chem Commun. 2000; 5: 339–340.

46. Fibbioli M, Bandyopadhyay K, Liu SG, Echegoyen L, Enger O, Diederich F, et al. Redox-active self-assembled monolayers for solid-contact polymeric membrane ionselective electrodes. Chem Mater. 2002; 14: 1721e1729.

47. Fouskaki M, Chaniotakis N. Fullerene-based electrochemical buffer layer for ion-selective electrodes. Analyst. 2008; 133: 1072.

48. Li J, Yin T, Qin W. An all-solid-state polymeric membrane Pb2+-selective electrode with bimodal pore C60 as solid contact. Anal Chim Acta. 2015; 876: 49–54.

49. Rius-Ruiz FX, Crespo GA, Bejarano-Nosas D, Blondeau P, Riu J, RiusFX. Potentiometric strip cell based on carbon nanotubes as transducerlayer: toward low-cost decentralized measurements. Anal Chem. 2011; 83: 8810–8815.

50. Hernández R, Riu J, Rius FX. Determination of calcium ion in sap using carbon nanotube-based ion-selective electrodes. Analyst. 2010; 135: 1979.

51. Crespo GA, Macho S, Rius FX. Ion-selective electrodes using carbon nanotubes as ion-to-electron transducers. Anal Chem. 2008; 80: 1316–1322.

52. Ampurdanés J, Crespo GA, Maroto A, Sarmentero MA, Ballester P, Rius FX. Determination of choline and derivatives with a solid-contact ion-selective electrode based on octaamide cavitand and carbon nanotubes. Biosensors and Bioelectronics. 2009; 25: 344–349.

53. Faridbod F. Cu2+-selective sensors based on a new ion-carrier and their application for the analysis of copper content in water samples. Int J Electrochem Sci. 2017; 12: 876–889.

54. Faridbod F, Davarkhah N, Karamdoust S. All solid sate potentiometric sensors for the measurement of paroxetine in pharmaceutical formulation. Int J Electrochem Sci. 2015; 10: 8308–8320.

55. Parra EJ, Crespo GA, Riu J, Ruiz A, Rius FX. Ion-selective electrodes using multi-walled carbon nanotubes as ion-to-electron transducers for the detection of perchlorate. Analyst. 2009; 134: 1905–1910.

56. Yuan D, AnthisAHC,Afshar MGh, Pankratova N, Cuartero M, CrespoGA, Bakker E. All-solid-state potentiometric sensors with a multiwalled carbon nanotube inner transducing layer for anion detection in environmental samples. Anal Chem. 2015; 87: 8640–8645.

57. Papp S, J. Kozma J, Lindfors T, Gyurcsányi RE. Lipophilic Multi-walled carbon Nanotube-based solid contact potassium ion-selective electrodes with reproducible standard potentials. A Comparative study. Electroanalysis. 2020; 32: 867–873.

58. Kozma J, Papp S, Gyurcsányi RE. Solid-contact ion-selective electrodes based on ferrocene-functionalized multi-walled carbon nanotubes. Electrochem Commun. 2021; 123: 106903.

59. Kałuża D, Jaworska E, Mazur M, Maksymiuk K, Michalska A. Multiwalled carbon nanotubes–poly(3-octylthiophene-2,5-diyl) nanocomposite transducer for ion-selective electrodes: raman spectroscopy insight into the transducer/membrane interface. Anal Chem. 2019; 91: 9010–9017.

60. Mousavi Z, Bobacka J, Lewenstam A, Ivaska A. Poly(3,4-ethylenedioxythiophene) (PEDOT) doped with carbon nanotubes as ion-to-electron transducer in polymer membrane-based potassium ion-selective electrodes. J Electroanal Chem. 2009; 633: 246–252.

61. Ardalani M, Shamsipur M, Besharati-Seidani A. A new generation of highly sensitive potentiometric sensors based on ion imprinted polymeric nanoparticles/multiwall carbon nanotubes/polyaniline/graphite electrode for sub-nanomolar detection of lead(II) ions. J Electroanal Chem. 2020; 879: 114788.

62. Hassan E, Amr AlO, Kamel Kh. Improved solid-contact nitrate ion selective electrodes based on multi-walled carbon nanotubes (MWCNTs) as an ion-to-electron transducer. Sensors. 2019; 19: 3891.

63. Padnya PL, Porfireva AV, Evtugyn GA, Stoikov II, Solid contact

potentiometric sensors based on a new class of ionic liquids on thiacalixarene platform. Front Chem. 2018; 6: 594.

64. Liu Y, Liu Y, Yan R, Gao Y, Wang P. Bimetallic AuCu nanoparticles coupled with multi-walled carbon nanotubes as ion-to-electron transducers in solid-contact potentiometric sensors. Electrochim Acta. 2020; 331: 135370.

65. Li F, Ye J, Zhou M, Gan S, Zhang Q, Han D, Niu L. All-solid-state potassium-selective electrode using graphene as the solid contact. Analyst. 2012; 137: 618–623.

66. Park HJ, Jeong JM, Yoon JH, Son SG, Kim YK, Lee KG, et al. Preparation of ultrathin defect-free graphene sheets from graphite via fluidic delamination for solid-contact ion-to-electron transducers in potentiometric sensors. J. Colloid Interface Sci. 2020; 560: 817–824.

67. Ping J, Wang Y, Wu J, Ying Y. Development of an all-solid-state potassium ion-selective electrode using graphene as the solid-contact transducer, Electrochem Commun. 2011; 13: 1529–1532.

68. Sun Q, Li W, Su B. Highly hydrophobic solid contact based on graphene-hybrid nanocomposites for all solid state potentiometric sensors with well-formulated phase boundary potentials. J Electroanal Chem. 2015; 740: 21–27.

69. Paczosa-Bator B. Ion-selective electrodes with superhydrophobic polymer/carbon nanocomposites as solid contact. Carbon NY. 2015; 95: 879–887.

70. Jaworska E, Lewandowski W, Mieczkowski J, Maksymiuk K, Michalska A. Critical assessment of graphene as ion-to-electron transducer for all-solid-state potentiometric sensors. Talanta. 2012; 97: 414–419.

71. Liu Y, Meng Z, Qin Y, Jiang D, Xi K, Wang P. Thiol-functionalized reduced graphene oxide as self-assembled ion-to-electron transducer for durable solid-contact ion-selective electrodes. Talanta. 2020; 208: 120374.

72. Hernández R, Riu J, Bobacka J, Vallés C, Jiménez P, Benito AM, et al. Reduced graphene oxide films as solid transducers in potentiometric all-solid-state ion-selective electrodes. J Phys Chem. 2012; 116: 22570–22578.

73. Ping J, Wang Y, Wu J, Ying Y. Development of an electrochemically reduced graphene oxide modified disposable bismuth film electrode and its application for stripping analysis of heavy metals in milk. Food Chem. 2014; 151: 65–71.

74. Boeva ZA, Lindfors T. Few-layer graphene and polyaniline composite as ion-to-electron transducer in silicone rubber solid-contact ion-selective electrodes. Sensors Actuators B Chem. 2016; 224: 624–631.

75. Abd-Rabboh HSM, Kamel AH, AmrAE-GE. All-solid-state calcium sensors modified with polypyrrol (PPY) and graphene oxide (GO) as solid-contact ion-to-electron transducers. Chemosensors. 2020; 8: 93.

76. Yang Q. All-solid-state Ca2+ion-selective electrode with black phosphorus and reduced grapheneoxide as the mediator layer. Int J Electrochem Sci. 2019; 14: 4933–4945.

77. Kim MY, Lee JW, Park DJ, Lee JY, Myung NV, Kwon SH, et al. Highly stable potentiometric sensor with reduced graphene oxide aerogel as a solid contact for detection of nitrate and calcium ions. J Electroanal Chem. 2021; 897: 115553.

78. Pięk M, Piech R, Paczosa-Bator B. All-solid-state nitrate selective electrode with graphene/tetrathiafulvalene nanocomposite as high redox and double layer capacitance solid contact. Electrochim Acta. 2016; 210: 407–414.

79. Tang W, Ping J, Fan K, Wang Y, Luo X, Ying Y, Wu J, Zhou Q. All-solid-state nitrate-selective electrode and its application in drinking water. Electrochim Acta. 2012; 81: 186–190.

80. Shvedene NV, Rzhevskaia AV, Anuchin NM, Kapitanova OO, Baranov AN, Pletnev IV. Reduced graphene oxide in the construction of solid-state bromide-selective electrode. J Anal Chem. 2015; 70: 378–383.

81. Jiang C, Yao Y, Cai Y, Ping J. All-solid-state potentiometric sensor using single-walled carbon nanohorns as transducer. Sensors Actuators B Chem. 2019; 283: 284–289.

82. Chai D, Sun Y, Li Zh,Yang H, Mao Sh, et al. A novel inorganic redox buffer of r-GO/Ag@AgCl/TMMCl utilized as an effective ion-to-electron transducer for a solid contact calcium ion-selective electrode. Sens. Actuators B Chem. 2022; 367: 132055.

83. Liang R, Yin T, Qin W. A simple approach for fabricating solid-contact ion-selective electrodes using nanomaterials as transducers. Anal Chim Acta. 2015; 853: 291–296.

84. Gadhari NS, Gholave JV, Patil SS, Patil VR, Upadhyay SS. Enantioselective high performance new solid contact ion-selective electrode potentiometric sensor based on sulphated γ-cyclodextrin-carbon nanofiber composite for determination of multichiral drug moxifloxacin. J Electroanal Chem. 2021; 882: 114981.

85. Rousseau CR, Bühlmann P. Calibration-free potentiometric sensing with solid-contact ion-selective electrodes. TrAC Trends Anal Chem. 2021; 140: 116277.

86. Arunachalam P. Polymer-based nanocomposites for energy and environmental applications. In: Polym. Nanocomposites Energy Environ. Appl. Elsevier. 2018; 185–203.

87. Trommer K, Petzold C, Morgenstern B. Processing and properties of carbon nanotube PVC composites. J Appl Chem. 2014; ID 307274: 1–10.

88. Broza G, Piszczek K, Schulte K, Sterzynski T. Nanocomposites of poly(vinyl chloride) with carbon nanotubes (CNT). Compos Sci Technol. 2007; 67: 890–894.

89. Seeponkai N, Wootthikanokkhan J, Thanachayanont C. Synthesis and characterization of fullerene functionalized poly(vinyl chloride) (PVC) and dehydrochlorinated PVC using atom transfer radical addition and AIBN based fullerenation. J Appl Polym Sci. 2013; 130: 2410–2421.

90. Joshi GM, Deshmukh K. Optimized quality factor of graphene oxide-reinforced PVC nanocomposite, J Electron Mater. 2014; 43: 1161–1165.

91. Francis E, Tippabattini J, Choi ES, Thomas S, Kim J. Morphology and dielectric properties of poly(vinyl chloride)-[multiwalled carbon nanotube-barium titanate] hybrid composite.In: V.K. Varadan (Ed.), 2017; 101671V.

92. Hussein MA, Alam A, Asiri AM, Al-amshany ZM, Hajeeassa KS, Rahman MM. Ultrasonic-assisted fabrication of polyvinyl chloride/mixed graphene-carbon nanotube nanocomposites as a selective Ag+ ionic sensor. J Comp Mat. 2019; 002199831882529.

93. Al NaimAbF, Al Fannakh H, Arafat S, Ibrahim SS. Characterization of PVC/MWCNTs nanocomposite: solvent blend. Sci Eng Compos Mater. 2020; 27: 55–64.

94. Skórczewska K, Lewandowski K, Wilczewski S. Novel composites of poly(vinyl chloride) with carbon fibre/carbon nanotube hybrid filler. Materials (Basel). 2022; 15: 5625.

95. Düzgün A, Zelada-Guillén GA, Crespo GA, Macho S, Riu J, Rius FX. Nanostructured materials in potentiometry. Anal Bioanal Chem.

2011; 399: 171–181.

96. Bakker E, Bühlmann Ph, Pretsch E. The phase-boundary potential model. Talanta. 2004; 63: 3–20.

97. Cuartero M, Bishop J, Walker R, Acres RG, Bakker E, De Marco R, Crespo GA. Evidence of double layer/capacitive charging in carbon nanomaterial-based solid contact polymeric ion-selective electrodes. Chem. Commun. 2016; 52: 9703–9706.

98. Turyshev ES, Kopytin AV, Zhizhin KYu, Kubasov AS, Shpigun LK, Kuznetsov NT. Potentiometric quantitation of general local anesthetics with a new highly sensitive membrane sensor. Talanta. 2022; 241: 123239.

99. Kubasov AS, Turishev ES, Kopytin AV, Shpigun LK, Zhizhin KYu, Kuznetsov NT. Sulfonium closo-hydridodecaborate anions as active components of a potentiometric membrane sensor for lidocaine hydrochloride. Inorg Chim Acta. 2021; 514: 119992.

100. Zhang D, Sun J, Lee LJ, Castro JM. Overview of ultrasonic assisted manufacturing multifunctional carbon nanotube nanopaper based polymer nanocomposites. Eng Sci. 2020.

101. Ashrapov AKh, Abdrakhmanova LA, Nizarov RK, Khosin VG. Development of effective ways of introducing nanofillers to PVC composites. Materials of RAACS XV workshop. Kazan. 2010; 272–278.

102. Bard AJ, Faulkner LR. Electrochemical Methods: fundamentals and applications (2nd ed.).In: John Wiley & Sons, New York, 2001.

103. Papakonstantinou P, Kern R, Robinson L, Murphy H, Irvine J, McAdams E, et al. Fundamental electrochemical properties of carbon nanotube electrodes.Fullerenes, Nanotub. Carbon Nanostructures. 2005; 13: 91–108.

104. Nasibulin AG, Pikhitsa PV, Jiang H, Brown DP, Krasheninnikov AV, Anisimov AS, et al. A novel hybrid carbon material. Nature Nanotechnology. 2007; 2: 156–161.

105. Smith BW, Monthioux M, Luzzi DE. Encapsulated C60 in carbon nanotubes. Nature. 1998; 396: 323–324.

106. Vizuete M, Barrejón M, Gómez-Escalonilla MJ, Langa F. Endohedral and exohedral hybrids involving fullerenes and carbon nanotubes. Nanoscale. 2012; 4: 4370.

107. Guldi DM, Menna E, Maggini M, Marcaccio M, Paolucci D, Paolucci F, et al. Supramolecular hybrids of fullerene and single-wall carbon nanotubes. Chem - A Eur J. 2006; 12: 3975–3983.

108. Lindner EY, Umezawa Y. Performance evaluation criteria for preparation and measurement of macro- and microfabricated ion-selective electrodes (IUPAC Technical Report). Pure Appl Chem. 2008; 80: 85–104.

109. VederJP, De Marco R, Clarke G, Chester R, Nelson A, Prince K, et al. Elimination of undesirable water layers in solid-contact polymeric ion-selective electrodes. Anal Chem. 2008; 80: 6731–6740.

110. Lindfors T, Sundfors F, Höfler L, Gyurcsányi RE. FTIR-ATR Study of water uptake and diffusion through ion-selective membranes based on plasticized poly(vinyl chloride). Electroanalysis. 2009; 21: 1914–1922.

111. Li Z, Li X, Rothmaier M, Harrison DJ. Comparison of numerical modeling of water uptake in poly(vinyl chloride)-based ion-selective membranes with experiment. Anal Chem. 1996; 68: 1726–1734.